

ELECTRIC FIELD MEASUREMENT IN GLOW DISCHARGE PLASMA INTERACTING WITH SHOCK WAVE IN HYPERSONIC FLOW

Nghia Cao Van¹, Hajime Itoh², Makoto Mizoguchi³ & Atsushi Uenaka⁴

¹Ph.D. Student, Aerospace Engineering, National Defense Academy of Japan
 ²Professor, Aerospace Engineering, National Defense Academy of Japan
 ³Associate Professor, Aerospace Engineering, National Defense Academy of Japan
 ⁴Japan Ground Self-Defense Force

Abstract

In this study, we investigated the impact of the existence of a physical probe on the electric potential along the positive column produced across a shock wave in hypersonic flow when using the floating probe method for plasma measurements. When the probe is inserted into the positive column behind the shock wave, the cross-sectional area of the positive column behind the shock wave becomes narrower than that in the uniform flow where the probe is not inserted, and also the brightness of the positive column behind the shock wave becomes stronger than that when the probe is not inserted. On the other hand, when the probe is inserted into the positive column in the uniform flow, there is no notable change in the appearance of the positive column. The probe measurements show that when the probe is inserted behind the shock wave, the measured reduced electric field is 3.75 times higher than that measured when the probe is inserted into the positive column in the uniform flow. Considering the changes of reduced electric field and the cross-sectional area of the positive column leads us to the conclusion that the electron number density does not change across the shock wave. The reason that the reduced electric field increases behind the shock wave in the probe measurements was elucidated.

Keywords: Hypersonic Flow, Shock Wave, Glow Discharge, Electric Field

1. Introduction

Visualizations and quantitative measurements are essential to elucidate the aerodynamic characteristics and the flow phenomena of the flows around hypersonic vehicles. Various methods have been proposed and used in hypersonic flows according to the purposes, environmental circumstances, and characteristics of each method. LIF [1], CARS [2], REMPI [3], and e-beam [4] are used to observe flow fields at the molecular level. However, generally, because of low signal intensities, these methods often require complex and expensive apparatus, long measurement times, and numerous trials. On the other hand, the glow discharge method, which our laboratory has focused on, has a high signal intensity and requires a relatively simple measurement system. Furthermore, the discharge method allows for three-dimensional visualization of flow fields [5]. The history of electrical discharge for visualizing flows is long, with the identification of shock wave shapes and flow velocity measurements being conducted. McCroskey et al. used the discharge to visualize shock waves and boundary layers around a flat plate model and showed that shock waves can be visualized even in rarefied conditions, where the Schlieren method does not work well [6]. Horstman et al. examined the characteristics of the flow fields around slender cones in the viscous interaction regime using a glow discharge [7]. Fisher et al. used a discharge to visualize a low-density supersonic free jet [8]. Kimura et al. attempted to visualize shock waves by utilizing the brightness of discharge fluorescence which depends on gas density [9]. Nishio and Itoh proposed a method to visualize three-dimensional shock wave shapes around hypersonic vehicles using an electric discharge [5]. Jiang et al. developed a glow discharge technique based on high-frequency excited power to visualize the rarefied flow field in

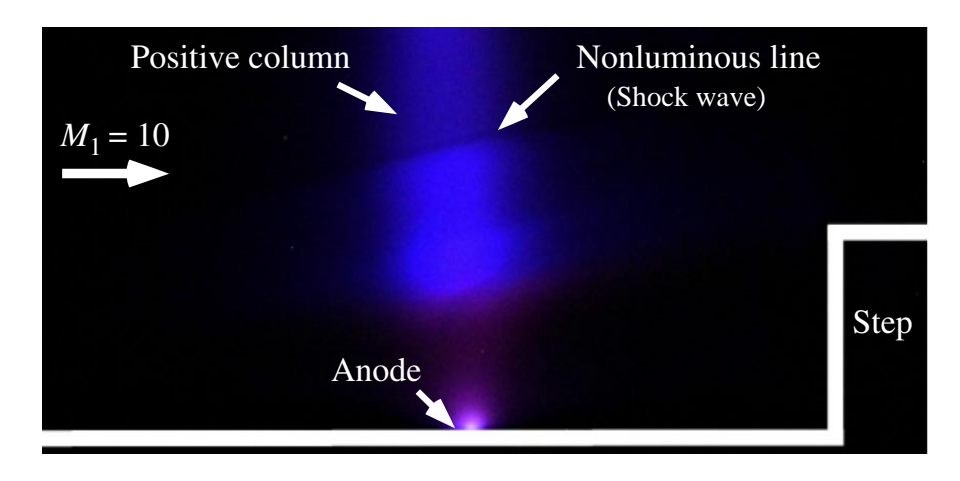


Figure 1 – Glow Discharge Visualizations of Flow past Forward-Facing Step [13]

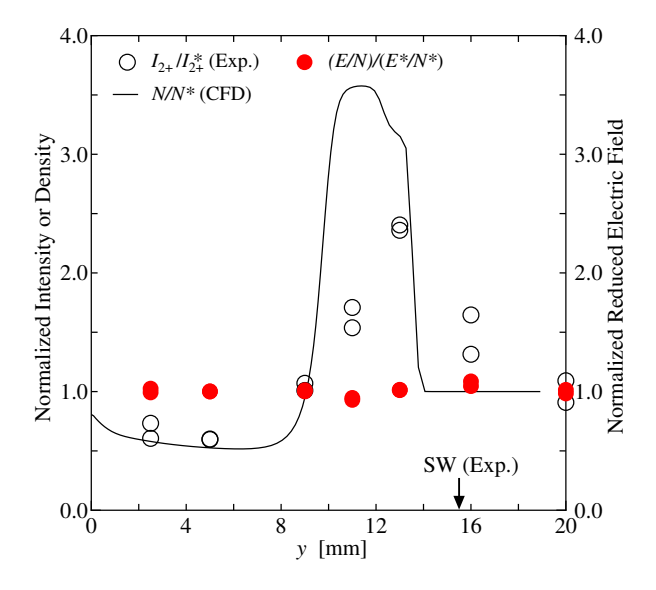


Figure 2 – Electric Field with Emission Intensity and Gas Number Density Distributions (Reproduced from article [13])

a Φ 1 m hypersonic low-density wind tunnel [10]. On the other hand, a few quantitative measurements using the discharge have been conducted. Itoh measured the velocity distribution within a hypersonic boundary layer using the glow discharge tracer method [11]. Stanfield et al. used the emission spectrum of discharges generated on the surface of a model to measure temperature in a boundary layer [12]. However, it is not enough to consider that the electrical discharge method can be adopted as a quantitative one for the measurement of hypersonic flows. We think that this situation is partly due to a lack of knowledge about the characteristics of the discharge plasma interacting with hypersonic flow.

A glow discharge plasma allows us to visualize and measure the flows with an emission intensity higher than that of the aforementioned methods. Therefore, this method enables visualization and measurement with a relatively short exposure time. For example, a pulse discharge of $2\mu s$ duration is bright enough to be captured by a commercial still camera. Figure 1 shows a flow field around a step model in a hypersonic flow under these discharge conditions (other conditions are described in detail in the following section). Furthermore, synchronized images taken by a high-speed camera can provide unsteady data with the necessary time resolution. As shown in Figure 1, the emission color and intensity of the positive column in the uniform flow and those behind the shock wave are different. These differences are considered to correspond to the changes in the flow state, but this characteristic has not been used much for quantitative measurements of flow.

The possibility of quantitative measurements of flow using electric discharges can be increased

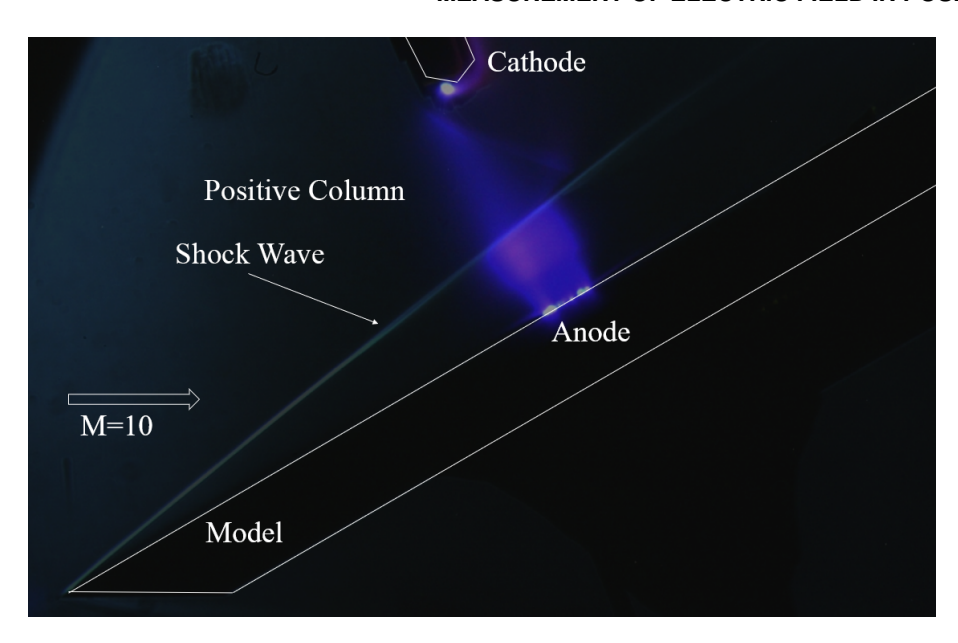


Figure 3 - Glow Discharge and Schlieren Visualizations of Flow around Flat Plate at Angle of Attack

by investigating how the emission spectrum and intensity respond to the changes in gas number density and temperature caused by shock waves. In a previous study [14], a qualitative explanation of the relationship among gas number density, emission intensity, and electric field in hypersonic flow was attempted. Itoh and Mizoguchi [13] specified the discharge type to glow discharge and considered the electronic excitation, and emission processes of molecules in the positive column to develop the following relation.

$$\frac{N^*}{N} = \left(\frac{E/N}{E^*/N^*}\right)^{6.05} \frac{I_{2+}^*}{I_{2+}} + \left[\left(\frac{E/N}{E^*/N^*}\right)^{6.05} \frac{I_{2+}^*}{I_{2+}} - 1\right] k_q \tau N^* \tag{1}$$

where N is the gas number density, E is the electric field strength, I_{2+} is the overall emission intensity of the second positive bands of nitrogen molecules, k_q is the overall quenching coefficient, τ is the emission lifetime of the second positive bands of nitrogen molecules, and superscript * denotes the values obtained at a reference point. With the reduced electric field assumed to be uniform in the positive column, the gas number density distribution is obtained through Equation 1 with the emission intensity distribution measured by spectroscopy in the flow field in Figure 1. This distribution agrees with that obtained from the CFD simulation. Therefore, the assumption that the reduced electric field is uniform is considered as reasonably valid. Figure 2 shows the reduced electric field distribution calculated through Equation 1 using the gas number density distribution from CFD simulation. The horizontal axis represents the distance from the anode bonded to the model surface, and the vertical axis represents the dimensionless emission intensity, gas number density, and reduced electric field. The white circles represent the emission intensity distribution measured by spectroscopy, the solid line represents the gas number density distribution from CFD simulation, the red circles represent the reduced electric field distribution, and SW indicates the position of the shock wave. The assumption that the reduced electric field within the positive column is uniform even when the gas number density changes in the positive column is considered a useful characteristic for us to interpret glow discharge measurement results quantitatively. Moreover, the condition itself is quite interesting, because it indicates that the electric field increases linearly with increasing gas number density. Especially, at the shock wave, the electric field should change discontinuously, which implies that there is a space charge layer there. This layer is available for shock wave visualization [15]. However, there is no concrete evidence to support the assumption except for the above argument. Therefore, to obtain positive proof of the assumption and clarify the cause, we used a floating probe method for electric field measurements of the positive column interacting with a flow field around a flat plate model, which is simpler than the flow field around the step model [16]. The visualization image of this flow is shown in Figure 3. However, the probe measurements showed that the reduced electric field

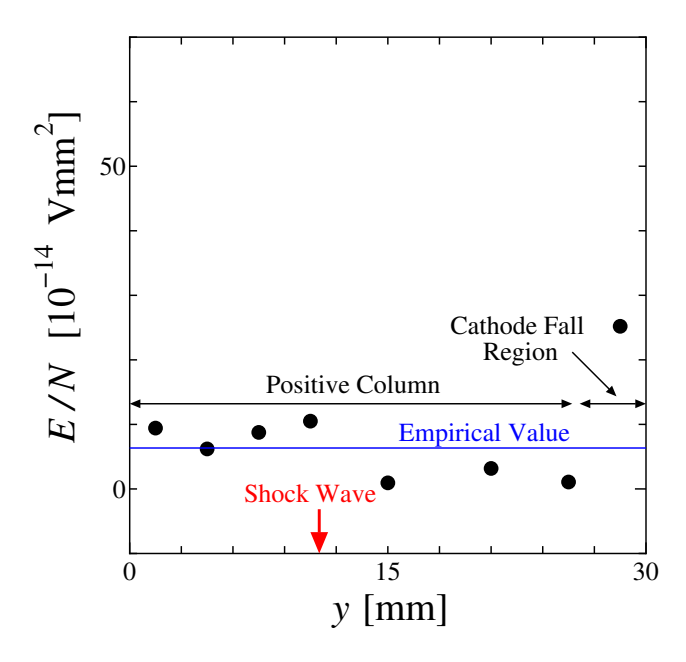


Figure 4 – Typical Results of Probe Measurements

changed discontinuously at the shock wave. Typical results of the probe measurements are shown in Figure 4. The horizontal axis represents the distance from the anode bonded to the model surface, and the vertical axis represents the reduced electric field. The black circles are the measured values and the solid blue line represents an empirical value in discharge tubes. Unlike the spectroscopic measurements, the probe measurements show that the reduced electric field increases behind the shock wave. The authors suggest that the difference between the probe measurement results and the argument of the spectroscopic measurement is possibly due to the insertion of the probe, the probe can distort the electron current. Therefore, in this paper, we investigate the impact of the probe insertion on the electric field along the positive column when using the floating probe method. To do that, we visualize the positive column interacting with the shock wave in hypersonic flow, with the probe inserted into it.

2. Experimental Setup

2.1 Hypersonic Gun Tunnel

The experiments were performed in the National Defense Academy (NDA) hypersonic gun tunnel, a schematic of which is shown in Figure 5, at a freestream Mach number of $M_1=10$. At the clamping section between the high- and low-pressure tubes (breech and barrel), a quick-opening valve was mounted instead of a metal diaphragm. The tunnel was equipped with a single-pass Schlieren system. Air was used as the test medium. The stagnation pressure was $p_0=2.0$ MPa, and the stagnation temperature was $T_0=760$ K, giving a freestream unit Reynolds number of $Re=2.5\times10^6$ m⁻¹ and a freestream number density of $N_1=0.95\times10^{17}$ molecules/cm³. The useful testing time was about 100 ms. A flow was generated through a conical nozzle with an expansion angle of 15° and an exit diameter of 180 mm. The streamwise Mach number deviation due to the conical flow effect was $\pm3\%$, which was determined through a pitot survey of the nozzle flow. For details on the hypersonic gun tunnel, please refer to article [13].

2.2 Test Model

To generate an oblique shock wave with a known density ratio, a flat plate model was used. The outline of the model is shown in Figure 6. The dimensions of the flat plate are 120 mm in length, 100 mm in width, and 10 mm in thickness, with the model's leading edge being a 30° wedge shape. The angle of attack of the model was set to be 30° . The leading edge of the model was placed 5 mm downstream from the nozzle exit. The material of the model was Bakelite, considering its machinability and electrical insulation properties.

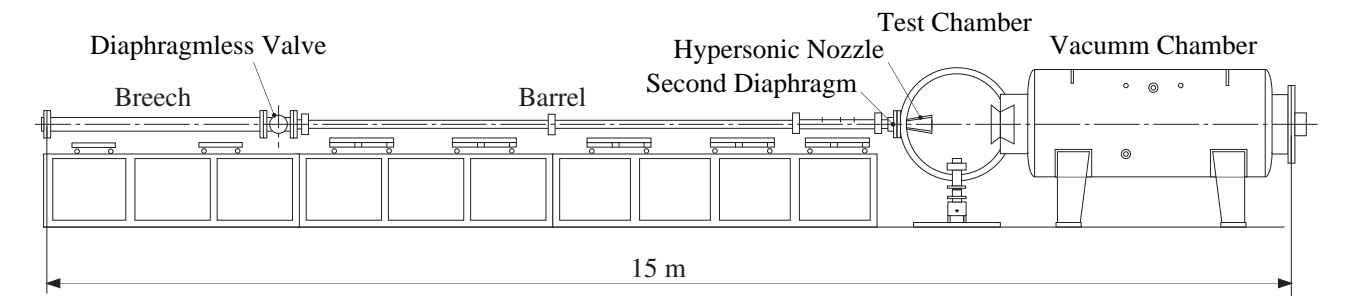


Figure 5 – Hypersonic Gun Tunnel

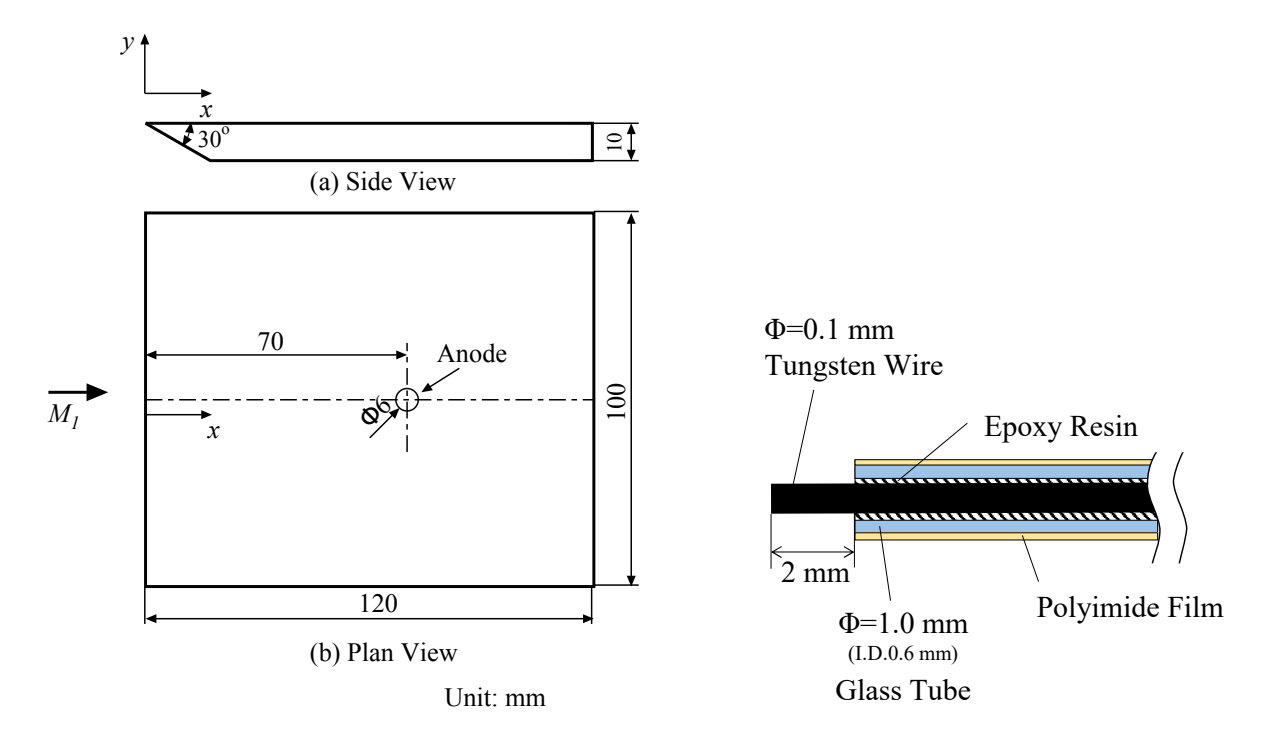


Figure 6 – Representation of the Test Model

Figure 7 – Probe Structure

In this study, the discharge column is generated between a cathode placed in the uniform flow and an anode flush with the model surface. When the anode on the model is a point one, the discharge column near it is known to taper toward it. This phenomenon is not desirable because the Equation 1 is derived under the assumption that the cross-sectional area of the positive column is uniform [13]. To avoid the changes in the cross-sectional area of the positive column as possible, a cylindrical copper anode with a diameter of 6 mm was installed on the flat plate model. A hole with the same diameter was drilled through the model, through which the cylindrical anode passed from the back of the model. It was connected to the anode of the transformer with a conductor wire. The arrangement of the anode is shown in Figure 6b. A tungsten cathode which is a rod with a diameter of 3 mm was placed 30 mm away from the model surface with its axis at a right angle to the surface and pointing the anode. So as not to disturb the flow field under observation, the gap between the electrodes was 30 mm. The tip of the cathode was shaped into a cone with a semi-apex angle of 30°. Except for the tip, the rod was wrapped with Kapton tape to insulate it from the plasma. The surfaces of the electrodes were cleaned of any debris at each shot.

2.3 Floating Probe Method

2.3.1 Priciples of Measurement

When a probe is inserted into the plasma, electrons and ions flow from the plasma toward the probe. In cold plasmas formed by discharges, the thermal velocity of electrons is much higher than that of ions, so that an excess of electrons reaches the probe. The probe potential then becomes

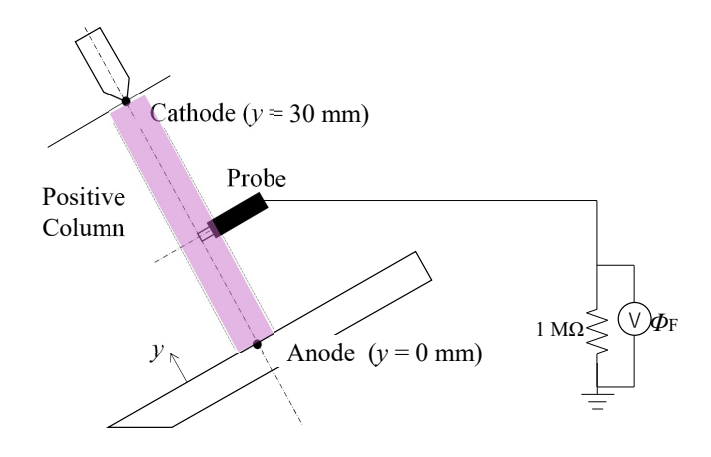


Figure 8 – Probe Setting

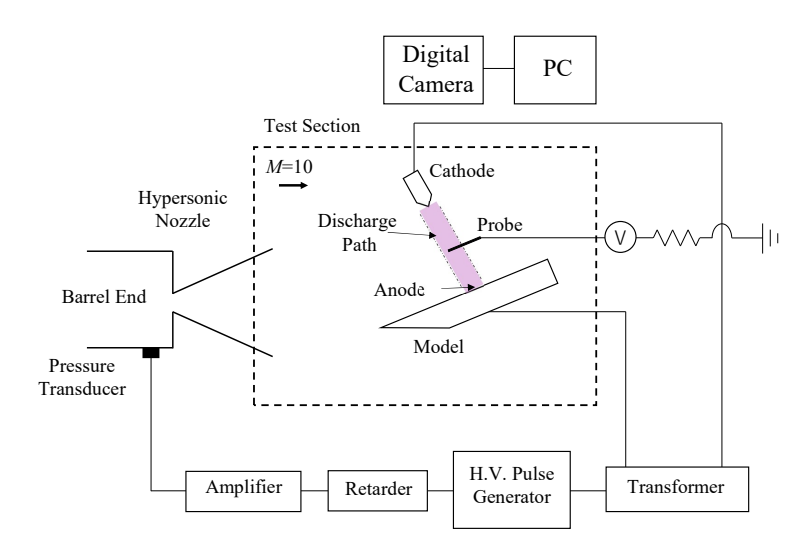


Figure 9 – Schematic of System for Visualizing Glow Plasma Interacting with Probe in Hypersonic Flow

negative concerning the plasma, driving back electrons and accelerating ions to form an ion sheath with the plasma so that the particle fluxes of electrons and ions are equal. When this ion sheath is formed, the potential of the probe is the floating potential. The distribution of potential and charged particle density when ion sheaths are formed are shown in Figure 11. The method of inserting a probe into the plasma to measure the local floating potential is called the floating probe method or the electrostatic probe method [17]. The probe is electrically isolated from the reference potential (which was set to ground in this experiment) by connecting a 1 M Ω resistor at the opposite end. The voltmeter reading taken in this state is the floating potential Φ_F . In the floating probe method, the floating potential is often measured by taking the cathode potential V_C as the reference potential. However, the cathode potential V_C in this discharge has a potential of 50-100 V and oscillations with an amplitude of 5-20 V_{P-P} . Using a V_C that fluctuates at a high potential as a reference potential may cause noise contamination and damage to the voltmeter. For this reason, in this study, the floating potential Φ_F was assumed to be the voltage between the probe and the reference potential (Earth).

2.3.2 Probe

The probe used in this study is shown in Figure 7. The conductive part of the probe was tungsten wire, which passed through a glass tube and bonded to the tube's inner wall using epoxy resin. The wire terminal was connected to a high-voltage transmission cable rated for a maximum of 20 kV-DC (UL3239GAWG22/20kV, length 4 m). The outer wall of the glass tube was covered with polyimide

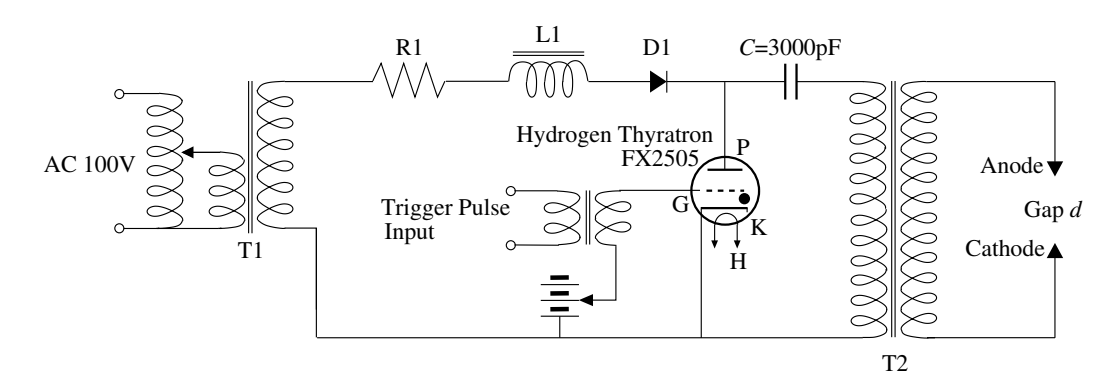


Figure 10 - Discharge Circuit

film. The high-voltage transmission cable was connected to measuring equipment located outside the wind tunnel measurement section. The probe-cable system was electrically insulated from the wind tunnel carefully. For details on the probe measurement, please refer to article [16]. The probe was set as shown in Figure 8.

2.4 Glow Discharge Method

Schematics of the experimental setup and the electrical discharge circuit are shown in Figures 9 and 10, respectively. A detailed description of the circuit has been presented in a previous paper [18]. When the hydrogen thyratron (FX2505) was switched on by an amplified pulse from the pressure transducer (PCB 111A24) at the downstream end of the low-pressure tube, the circuit was completed, and the capacitor discharged across the electrode gap through transformer T2, whose turn ratio was 2.75. By using a retarder, the pulse producing the discharge was delayed until the freestream was being generated. A high-voltage pulse with a duration of 2 μ s supplied by the circuit was applied to the gap to generate the glow discharge across the shock wave forming at the leading edge of the model. An energy storage capacitor in the circuit was charged to 2.8 kV by a high-voltage supply. A capacitance of 3000 pF was carefully selected as a compromise between the light requirement for photographic purposes and the reduction of disturbances due to added electrical energy, which was several millijoules. The emission intensity produced per pulse allows the use of a commercial, digital single-lens reflex still camera with a simple optical system [19].

2.5 Digital Camera

For visualizing the glow discharge produced in the hypersonic flow, a CANON EOS-1D camera and a 105 mm lens with an f-number of 1.4 were used. The camera was placed outside the wind tunnel measurement section and 1 m apart from the model. The ISO sensitivity of the camera was set to 3200. The resolution of the image was 12 pixels/mm.

3. Results and Discussion

To provide a better comparison of the appearances of positive columns with and without the probe inserted, glow discharge visualizations were conducted under the same conditions except for the presence of the probe. The RAW images obtained by the camera were converted to TIFF images as follows to prevent the brightness and color information on the RAW images from being lost. For converting RAW images, Canon Utilities RAW Image Converter Ver.2.0.2 was used. The conversion method chosen in the software was 'Linear'. Camera manual claims that this method performs a linear transformation with respect to the brightness of each pixel [20].

3.1 Positive Column without Probe Insertion

To investigate the influences that the positive column receives from the probe, firstly we visualize the positive column without the probe insertion both in a stationary air environment and in the flow. In stationary air, we set the pressure to 390 Pa to obtain the gas number density equal to that in the uniform flow. The visualization images of these cases are shown in Figures 12 and 13. In Figure 13, the positive column in the flow is brighter than that in the stationary air (Figure 12) and the shock wave

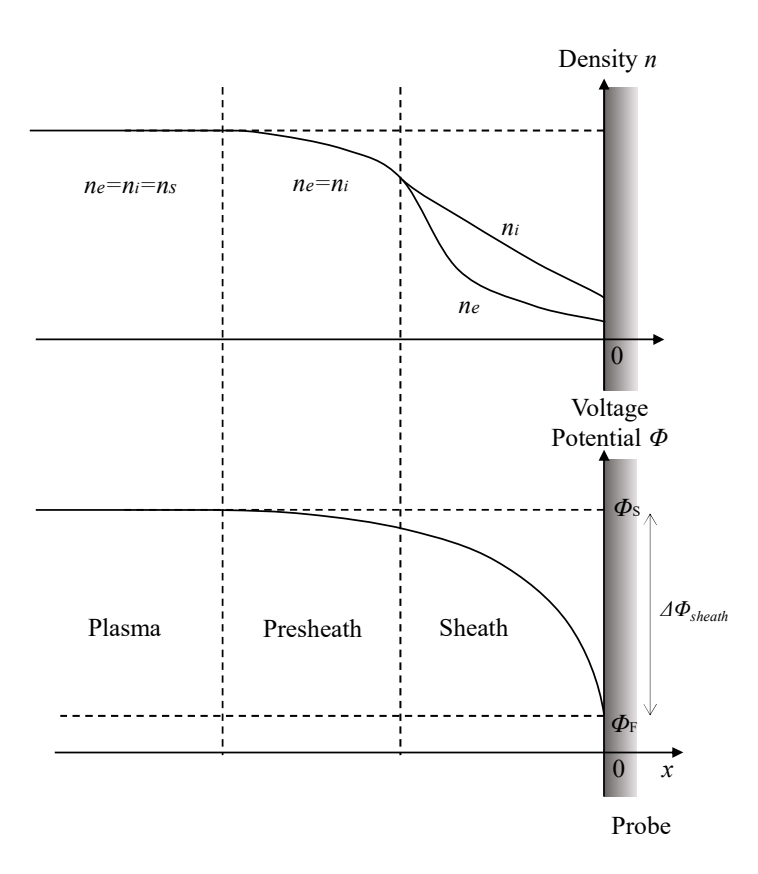


Figure 11 – Charged Paticles Density and Potential Distribution during Sheath Formation

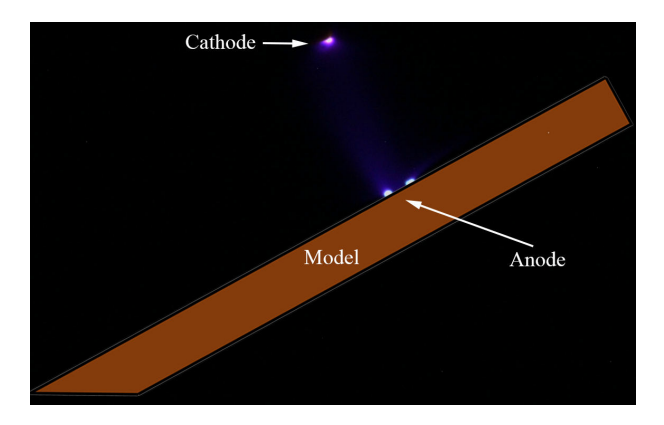
can be observed because of the difference in brightness and color in the regions in front of and behind it. The location of the shock wave is approximately at $y=10\,$ mm, which agrees with the position confirmed by Schlieren image. The shape of the positive column is assumed as a cylinder column. In this study, we focus on the change in the cross-sectional area of the positive column at the position of the shock wave. To obtain its diameter distribution, lines perpendicular to its axis are drawn as shown in Figure 14, and then RGB distributions along these lines are evaluated. The diameter of the positive column is determined through the B distribution. In Figure 13, the diameters of the positive column are the same in the uniform flow and behind the shock wave and approximately 17 mm. In stationary air, the diameter also does not change along the positive column and is approximately 14 mm.

3.2 Influences of the Probe Insertion in Stationary Air

To observe the influences of the probe insertion on the positive column under the stationary condition, Figure 15 visualizing the positive column with the probe insertion is compared with Figure 12 visualizing that without the probe insertion. The presence of the probe does not impact the appearance (shape and brightness) of the positive column and the probe measurement shows that the electric field is almost unchanged along the positive column except for a cathode fall region, and approximately $1.4\times10^{-14}~\rm Vmm^2$ [16], which is the same order of magnitude as a value (6.1 $\times10^{-14}~\rm Vmm^2$) empirically observed in glass tube experiments [21]. From the above arguments, we conclude that in this case, the probe does not impact the positive column.

3.3 Influences of the Probe Insertion in Hypersonic Flow

To investigate the influences of the probe insertion on the positive column in the uniform flow, we compare the visualization image of this case (Figure 16) to that without the probe insertion (Figure 13). When the probe is inserted into the positive column in the uniform flow, the appearance of the positive column is not significantly different from that observed without the probe insertion. Therefore,



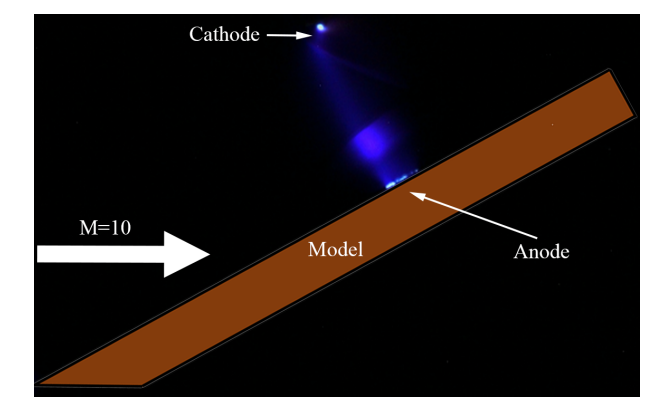


Figure 12 – Positive Column without Probe Insertion in Stationary Air

Figure 13 – Positive Column without Probe Insertion in Flow

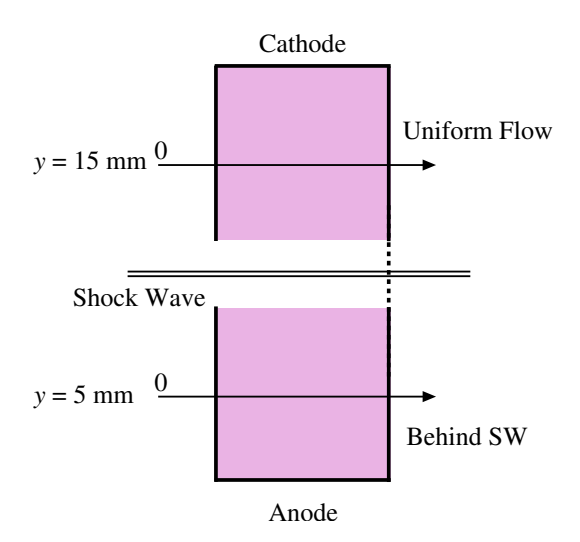


Figure 14 – Reading RGB Distributions in Positive Column

we can infer that the reduced electric field measured with the probe insertion in the uniform flow represents the value of the positive column without the probe insertion which is impossible to be measured by a conventional method. The value measured in the uniform flow is 2×10^{-14} Vmm² [16]. This value matches that measured with the probe inserted into the positive column in the stationary condition mentioned in the previous section.

To investigate the influences of the probe insertion on the positive column behind the shock wave, we compare the visualization image of this case (Figure 17) to that without the probe insertion (Figure 13). When the probe is inserted into the positive column behind the shock wave, the diameter of the positive column behind the shock wave is noticeably smaller than that in the uniform flow, and the brightness of the narrower region is lighter than that when the probe is not inserted (Figure 13). This phenomenon does not occur when the probe is inserted into the positive column in the uniform flow. From this observation, whether the phenomenon does occur or not likely depends on the gas number density. The reason can be explained as follows. In the region behind the shock wave of the positive column, the high gas number density can act as a resistance against the movement of the electrons, while the tungsten probe can function as a conductor. Consequently, the electrons tend to stop by the probe on the way from the cathode to the anode, resulting in the positive column behind the shock wave being narrower than that in the uniform flow. On the other hand, when the probe is set into the positive column in the uniform flow region, the gas number density there is low enough for the electrons to make a beeline toward the anode.

From the RGB distributions evaluated in Figure 17, the diameter of the positive column behind the shock wave is decreased by 1.4 times compared to the one in the uniform flow. We illustrate the change in the cross-sectional area of the positive column as shown in Figure 18, where numbers

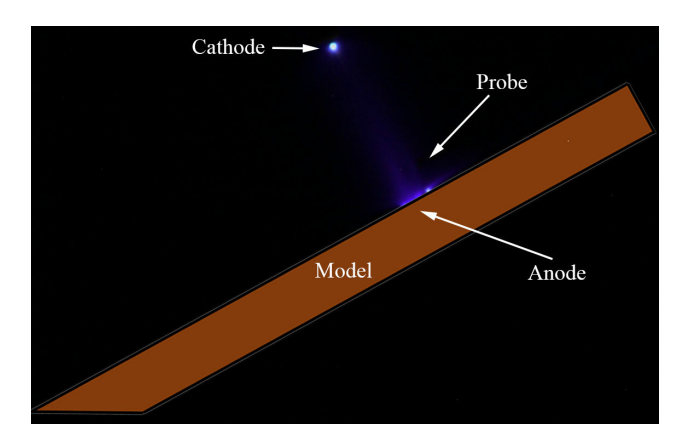


Figure 15 – Positive Column with Probe Inserted at y = 6 mm in Stationary Air

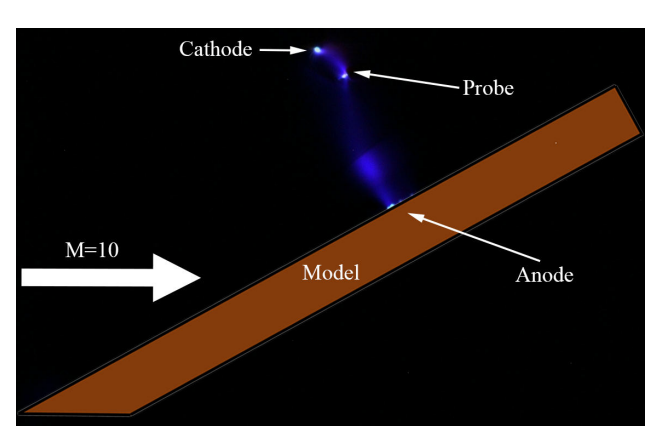


Figure 16 – Positive Column with Probe Inserted at y = 24 mm in Flow

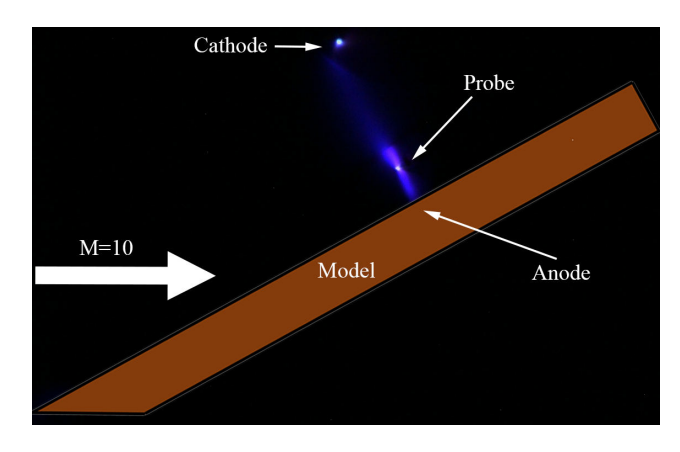


Figure 17 – Positive Column with Probe Inserted at y = 6 mm in Flow

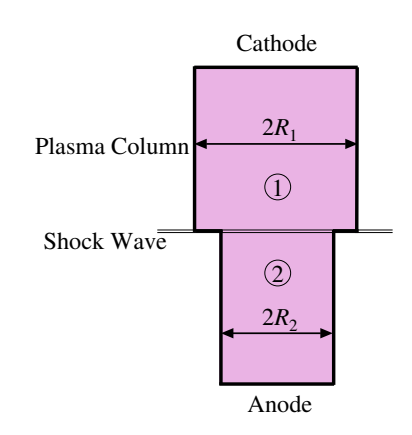


Figure 18 – Change in Cross Sectional Area

1 and 2 indicate the uniform flow and the flow behind the shock wave, R denotes the radius of the cross-sectional area of the positive column. In this illustration, the continuity equation for electrons is

$$n_{e1}v_{e1}A_1 = n_{e2}v_{e2}A_2, (2)$$

where n_e denotes the electron number density, v_e denotes the electron drift velocity depending on the reduced electric field E/N, and A denotes the cross-sectional area of the positive column. The empirically determined drift velocity for air is $v_e \propto (E/N)^{0.664}$, which is extracted from reference [22]. Substituting this relation into Equation (2), we obtain:

$$\left(\frac{E_2/N_2}{E_2/N_2}\right)^{0.664} = \frac{n_{e2}}{n_{e1}} \frac{R_2}{R_1} \tag{3}$$

From probe measurements, we have obtained the ratio $(E_2/N_2)/(E_1/N_1)=3.75$. Substituting this into Equation (3), we found $n_{e1}/n_{e2}\approx 1$. The electron number density in front of and that behind the shock wave seem to have a similar value. Applying this hypothesis to the continuity equation for electrons with a constant cross-sectional area assumed, it is concluded that the strength of the reduced electric field on the uniform flow side and that on the rear side of the shock wave are equal. Consequently, the difference between the results of the two measurement methods mentioned in the Introduction section can be explained without contradiction.

4. Conclusions

This study investigated the influence of probe insertion on the positive column interacting with the shock wave in hypersonic flow when using the floating probe method to measure plasmas. By considering the change in the cross-sectional area of the positive column, we elucidated the cause of the discrepancy between the reduced electric field measured with the floating probe method and that through the spectroscopic method in a previous study. Our findings suggest that the electron number density in front of and that behind the shock wave appear to be the same, which leads to the uniform reduced electric field along the positive column whose cross-sectional area is uniform.

References

- [1] Hanson, R., "Laser-Based Diagnostics for Hypersonic Flows," *New Trends in Instrumentation for Hypersonic Research*, Springer, 1993, pp. 185–194.
- [2] Exton, R., "Absorption, Scattering, and Fluorescence Techniques for Hypersonic Flow Measurements," *New Trends in Instrumentation for Hypersonic Research*, Springer, 1993, pp. 205–214.
- [3] Meier, U., Plath, I., and Kohse-Höinghaus, K., "Determination of Minority Species Concentrations and Temperature in Combustion Systems by Laser-Induced Fluorescence," *New Trends in Instrumentation for Hypersonic Research*, Springer, 1993, pp. 195–204.
- [4] Muntz, E. and Erwin, D., "Rapid Pulse Electron Beam Fluorescence for Flow Field Diagnostics," *New Trends in Instrumentation for Hypersonic Research*, Springer, 1993, pp. 265–273.
- [5] Nishio, M. and Itoh, H., "Second Electric Discharge Method for Visualizing Three-Dimensional Shock Shapes around Hypersonic Vehicles," *Transactions of the Japan Society for Aeronautical and Space Sciences*, Vol. 38, No. 119, 1995, pp. 38–45.
- [6] McCroskey, W., Bogdonoff, S., and McDougall, J., "An Experimental Model for the Sharp Flat Plate in Rarefied Hynersonic Flow," *AIAA Journal*, Vol. 4, No. 9, 1966, pp. 1580–1587.
- [7] Horstman, C. and Kussoy, M. I., "Hypersonic Viscous Interaction on Slender Cones." *AIAA Journal*, Vol. 6, No. 12, 1968, pp. 2364–2371.
- [8] Fisher, S. and Bharathan, D., "Glow-Discharge Flow Visualization in Low-Density Free Jets," *Journal of Spacecraft and Rockets*, Vol. 10, No. 10, 1973, pp. 658–662.
- [9] Kimura, T., Nishio, M., Fujita, T., and Maeno, R., "Visualization of Shock Wave by Electric Discharge," *AIAA Journal*, Vol. 15, No. 5, 1977, pp. 611–612.
- [10] Jiang, W., Qiu, H., Yang, Y., Shi, Y., Wang, J., Li, J., Long, Z., and Mao, C., "High Frequency AC Electric Glow Discharge Visualization Technology and Application in Big Diameter Hypersonic Low-Density Wind Tunnel," *Advances in Aerodynamics*, Vol. 3, No. 14, 2021.
- [11] Itoh, H., "Glow Discharge-Tracer Technique for Velocity Profile Measurement in Hypersonic Boundary Layer Flows," *Journal of the Japan Society for Aeronautical and Space Sciences*, Vol. 53, No. 615, 2005, pp. 154–159 (in Japanese).
- [12] Stanfield, S., Menart, J., Shang, J., Kimmel, R., and Hayes, J., "Application of a Spectroscopic Measuring Technique to Plasma Discharge in Hypersonic Flow," *AIAA Paper 2006-559*, 2006.
- [13] Itoh, H. and Mizoguchi, M., "Potential of Glow-Discharge Flow Measurement in Hypersonic Low-Density Flows," *AIAA Journal*, Vol. 58, No. 1, 2020, pp. 291–303.
- [14] Nishio, M. and Itoh, H., "A Qualitative Theory for Visualizing Three Dimensional Shock Waves around Hypersonic Vehicles Using Electric Discharge," *Transactions of the Japan Society for Aeronautical and Space Sciences*, Vol. 37, No. 117, 1994, pp. 208–216.
- [15] Itoh, H., "On the Shock Wave Visualization in Hypersonic Flows Using Glow Discharge," *Japan Society of Aeronautical Space Sciences*, Vol. 51, No. 598, 2003, pp. 647–649 (in Japanese).
- [16] Uenaka, A., "Probing of Discharged Plasma Generated for Hypersonic Flow Measurement," Master's Thesis, National Defense Academy of Japan, 2023 (in Japanese).
- [17] Lee, M. H., Jang, S. H., and Chung, C. W., "Floating Probe for Electron Temperature and Ion Density Measurement Applicable to Processing Plasmas," *Journal of Applied Physics*, Vol. 101, No. 3, 2007.
- [18] Itoh, H. and Mizoguchi, M., "On the Characteristics of an Electric Discharge Generated Across a Shock Wave in a Hypersonic Flow," *Journal of the Japan Society for Aeronautical and Space Sciences*, Vol. 51, No. 599, 2003, pp. 653–658 (in Japanese).
- [19] Itoh, H. and Mizoguchi, M., "Method for Visualizing Viscous Interaction in Hypersonic Low-Density Flows Using Electrical Discharge," *Journal of Spacecraft and Rockets*, Vol. 54, No. 1, 2017, pp. 225–232.
- [20] CANON, "RAW Image Processing, Viewing and Editing Software Digital Photo Professional Ver. 4.14 Instruction Manual," 2021.

- [21] Raizer, Y. P., Gas Discharge Physics, Springer, 1991.
- [22] Brown, S. C. and Singer, S., *Basic Data of Plasma Physics*, The Technology Press of the Massachusetts Institute of Technology, Cambridge; Wiley, New York; and Chapman and Hall, London, 1959, pp. 47–98.

Copyright Statement

The authors confirm that they, and/or their company or organization, hold copyright on all of the original material included in this paper. The authors also confirm that they have obtained permission, from the copyright holder of any third party material included in this paper, to publish it as part of their paper. The authors confirm that they give permission, or have obtained permission from the copyright holder of this paper, for the publication and distribution of this paper as part of the ICAS proceedings or as individual off-prints from the proceedings.